

Thermal quantum Simulation of the Schwinger model

Xu-Dan Xie,¹ Hong-Xi Xing,¹ Dan-Bo Zhang,^{1,*} and Zheng-Yuan Xue^{1,†}

1

(Dated: April 14, 2022)

In nuclear physics the concept that confinement of particles due to strong interaction can be diminished at high temperature is one key to understand the phase diagram of QCD. However, it is hard to solve equilibrium states of QCD systems at finite temperatures and finite densities. In this paper, using the one-dimensional Schwinger model, we show how to achieve the goal on a quantum computer, by preparing thermal states with variational quantum algorithms. We adopt a product ansatz from which the entropy and thus the free energy can be readily evaluated. The string tension, an indicator of confinement, then can be calculated as free-energy difference with/without a pair of opposite charges at two ends of the chain. We show that the string tension decreases exponentially at large temperatures, and the critical temperature becomes smaller for larger density. Our work paves a way for exploiting near-term quantum computers to study temperature induced deconfinement for nuclear matters.

I. INTRODUCTION

In theoretical physics, it is a important study project to understand the phase diagram of QCD. The confinement of particles due to strong interaction can be diminished at high temperature is one key to understand the phase diagram of QCD.

Recent research on the quantum computer has attracted a lot of attention. Theoretically, the universal quantum computer can efficiently solve problems that classical computers cannot efficiently solve such as large number decomposition [1], data search [2] and quantum simulation [3]. Due to the technical limitation, we are still some way from achieving the universal quantum computer. How to make good use of the current noisy intermediate-scale quantum (NISQ) device [8] is a critical issue and also a research hotspot in the field of quantum computing. The hybrid quantum-classical algorithm is considered one of the algorithms most likely to be implemented on near-term NISQ devices. With the help of classical computers, hybrid quantum-classical algorithms are able to utilize the capabilities of NISQ computing device to solve specific problems. In hybrid quantum-classical algorithms, parameterized quantum neural network is designed in quantum computer, and then the classical computer is used to minimize the loss function designed for a specific problem. After iterative optimization, our goal is obtained on quantum computer. Hybrid quantum-classical algorithms are widely applied in many fields, among which the most representative ones are quantum approximate optimization algorithm [13] for combinatorial optimization problems and variational quantum eigensolver for ground state energy problems. [10, 14] Hybrid quantum classical algorithms also have important applications in quantum simulation. Gibbs state is a key step in quantum simulation, multi-body physics research and many other fields. Using hybrid quantum-classical algorithm, gibbs state of given Hamiltonian can be prepared on a quantum computer. []

II. SCHWINGER MODEL

In physics, the Schwinger model is a testbed for the study of quantum gauge field theories, which describes the quantum electrodynamics in 1+1D (1 spatial dimension +time). In the temporal gauge, where the temporal component of the vector potential is set to zero, $A_0(x) = 0$, the Hamiltonian density of the continuum model reads

$$\hat{H} = \int dx \left[\Psi^\dagger(x) \gamma^0 \gamma^1 (-i\partial_1 + g\hat{A}_1(x)) \Psi(x) + m\Psi^\dagger(x) \gamma^0 \Psi(x) + \frac{1}{2} \hat{E}^2(x) \right], \quad (1)$$

where $\Psi(x)$ is a flavourless fermion field and \hat{A}_1 is the longitudinal vector potential. In 1+1D quantum electrodynamics, the Dirac matrices read $\gamma^0 = \hat{\sigma}^z$ and $\gamma^1 = i\hat{\sigma}^y$. According to the Maxwell's equations, the electric field satisfies $\hat{E}(x) = -\partial_0 A_1(x)$ and the commutation relation $[\hat{A}_1(x), \hat{E}(x')] = -i\delta(x - x')$. Here, $\hat{E}(x)$ can be interpreted as a background field.

To obtain a mapping from the the continuum physical picture to a lattice formulation, the staggered lattice approach is applied, which allows the field theory to be recast on a lattice, with lattice constant a . The relationship between lattice and continuum fields is $\hat{\Phi}_{2j} = \sqrt{a}\hat{\Psi}_e(x_{2j})$ for even lattice sites and $\hat{\Phi}_{2j-1} = \sqrt{a}\hat{\Psi}_e^+(x_{2j-1})$ for odd lattice sites. The gauge fields and electric fields also have lattice equivalents, $\theta_{j,j+1} = -agA(x_j + \frac{a}{2})$ and $L_{j,j+1} = \frac{1}{g}E(x_j + \frac{a}{2})$, where the fields $\theta_{j,j+1}$ and $L_{j,j+1}$ live on the links of the lattice and still keep the the commutation relation $[\theta_{j,j+1}, L_{j',j'+1}] = -i\delta_{j,j'}$. Thus, we get the Kogut-Susskind formulation of the the Schwinger model

$$\hat{H} = \frac{1}{2a} \sum_{j=1}^{N-1} [\hat{\Phi}_j^\dagger \hat{U}_{j,j+1} \hat{\Phi}_{j+1} + h.c.] + m \sum_{j=1}^N (-1)^j \hat{\Phi}_j^\dagger \hat{\Phi}_j + \frac{g^2 a}{2} \sum_{j=1}^{N-1} \hat{L}_j^2, \quad (2)$$

in which $\hat{U}_{j,j+1} = e^{i\theta_{j,j+1}}$ and N is the length of the lattice system.

* dbzhang@m.scnu.edu.cn

† zyxue@scnu.edu.cn

Gauss' law appears as the additional constraint,

$$\hat{L}_{j,j+1} - \hat{L}_{j-1,j} = \hat{\Phi}_j^\dagger \hat{\Phi}_j - \frac{1 - (-1)^j}{2}. \quad (3)$$

Consider an open boundary conditions, the gauge field at the boundary $\hat{L}_{0,1} = \varepsilon$, so

$$\hat{L}_{j,j+1} = \varepsilon + \sum_{l=1}^j \left[\hat{\Phi}_l^\dagger \hat{\Phi}_l - \frac{1 - (-1)^l}{2} \right] \quad (4)$$

This equation determines the electric field up to a constant ε_0 which can be added to $\hat{L}_{j,j+1}$ and represents the background electric field. In addition, with a gauge transformation of the fermi fields, $\hat{\Phi}_j \rightarrow \prod_{l=1}^{j-1} \hat{U}_{l,j+1} \hat{\Phi}_j$, the $\hat{U}_{l,j+1}$ in Eq.(2) is remove from the Hamilton. After such a transformation, the Hamilton of the model reads

$$\begin{aligned} \hat{H} = & \frac{1}{2a} \sum_{j=1}^{N-1} [\hat{\Phi}_j^\dagger \hat{\Phi}_{j+1} + h.c.] + m \sum_{j=1}^N (-1)^j \hat{\Phi}_j^\dagger \hat{\Phi}_j \\ & + \frac{g^2 a}{2} \sum_{j=1}^{N-1} \left(\varepsilon + \sum_{l=1}^j \left[\hat{\Phi}_l^\dagger \hat{\Phi}_l - \frac{1 - (-1)^l}{2} \right] \right)^2 \end{aligned} \quad (5)$$

Furthermore, the one component fermion fields can be replaced by Pauli spin operators via a Jordan-Wigner transformation, $\hat{\Phi}_j = \prod_{l=1}^{j-1} (i\sigma_l^z) \sigma_j^-$, where $\sigma^\pm = \sigma^x \pm i\sigma^y$. After the Jordan-Wigner transformation, the model can be mapped to a spin Hamiltonian

$$\begin{aligned} \hat{H}_\varepsilon = & \frac{1}{2a} \sum_{j=1}^{N-1} [\hat{\sigma}_j^+ \hat{\sigma}_{j+1}^- + h.c.] + \frac{m}{2} \sum_{j=1}^N (-1)^j \hat{\sigma}_j^z \\ & + \frac{g^2 a}{2} \sum_{j=1}^{N-1} \left(\varepsilon + \sum_{l=1}^j (\hat{\sigma}_l^z + (-1)^l) \right)^2 \end{aligned} \quad (6)$$

If we put a charge $-gQ$ at site 0 and a opposite charge $+gQ$ at site N as probe charges, we can absorb the probe charges into a background electric field string that connects the two sites. Using a quark with charge $g\varepsilon$ and an antiquark with charge $-g\varepsilon$ as the probe charge, it can be translated to a uniform background field $g\varepsilon$ in Hamilton of Eq(6). The "string tension", is defined as the increase in vacuum energy per unit length due to the external sources. From partition function $Z_\varepsilon(\beta) = \text{tr}(e^{-\beta H_\varepsilon})$, the string tension at finite temperature T is given by

$$\begin{aligned} \sigma_\varepsilon(\beta) &= \frac{1}{2N} \frac{1}{\beta} \log \left(\frac{Z_\varepsilon(\beta)}{Z_0(\beta)} \right) \\ &= \frac{1}{2N} (F_\varepsilon(\beta) - F_0(\beta)) \end{aligned} \quad (7)$$

where $\beta = \frac{1}{T}$ is the inverse temperature and $F_\varepsilon(\beta) = -\frac{1}{\beta} \log(Z_\varepsilon(\beta))$ is free energy of the system. In equilibrium thermodynamics, the free energy has another form

$$F_\varepsilon(\beta) = E_\varepsilon(\beta) - TS_\varepsilon(\beta), \quad (8)$$

where $E_\varepsilon(\beta) = \text{tr}(\hat{\rho}_\varepsilon(\beta))$ is the energy and the $S_\varepsilon(\beta) = -\text{tr}(\hat{\rho}_\varepsilon(\beta) \log(\hat{\rho}_\varepsilon(\beta)))$ is the entropy of system. The $\hat{\rho}_\varepsilon(\beta) =$

$\frac{1}{Z} e^{-\beta H_\varepsilon}$ is the Gibbs state describing the system in thermal equilibrium. If we want to attain the free energy of the system with large size N , we will face with a huge obstacle because the computation complexity has a exponential growth with N . It is a natural idea to use quantum computer to deal with quantum many-body problem. In this paper, we propose a quantum algorithm which can compute the free energy conveniently.

III. A QUANTUM VARIATIONAL ALGORITHM FOR GENERATING QUANTUM THERMAL STATES

In this section, we first introduce the initial state and the unitary neural network used in quantum computer. Then the procedure of the whole algorithm is presented in detail.

A. Initial state design

We now present our algorithm which can be used for generating quantum thermal states. In a quantum algorithm, initial state design is a very important step. The simpler the initial state preparation process is, the easier the algorithm is to implement, especially in NISQ(Noisy Intermediate-Scale Quantum computers). First, consider a quantum system which consists of N subsystems which are uncorrelated. The mixed state of each subsystem has the form

$$\rho_i(\theta_i) = \sin^2(\theta_i)|0\rangle\langle 0| + \cos^2(\theta_i)|1\rangle\langle 1|, \quad (9)$$

in which θ_i is variational parameter. Such a mixed state with a variational parameter θ_i is prepared through a simple quantum circuit(see Appendix A). With a small dimension, it is not difficult to figure out the Von Neumann entropy of the mixed state of the subsystems. According to the formula of von Neumann entropy, the entropy of the mixed state of the subsystems is given by

$$\begin{aligned} S_i(\rho_i) &= -\text{tr}[\rho_i \log(\rho_i)] \\ &= -\sin^2(\theta_i) \log[\sin^2(\theta_i)] - \cos^2(\theta_i) \log[\cos^2(\theta_i)]. \end{aligned} \quad (10)$$

From the above expression, we see that if ρ_i is specific, the entropy can be figured out directly. All subsystems are independent, hence the mixed state of the quantum system is the tensor product of the mixed state of the subsystems

$$\rho_{pro}(\theta) = \otimes_{i=1}^N \rho_i(\theta_i), \quad (11)$$

which we call it product state. Due to the tensor product structure, the Von Neumann entropy of the total quantum system become the sum of the entropy of the subsystems

$$\mathcal{S}(\rho_{pro}(\theta)) = \sum_i^N S_i(\rho_i(\theta_i)). \quad (12)$$

This sum decomposition is useful when estimating the expected value of the entropy of the total system. Compared with computing the entropy of a mixed state in 2^N -dimensional Hilbert space, it is much simpler to compute

the sum of the entropies of N mixed states in 2-dimensional Hilbert space. From Eq.(10) and Eq.(12), we can see that the entropy of the total system is only determined by the variational parameter set $\{\theta_i\}$. So far, we prepare a product state as the initial state parameterized by the variational parameter set $\{\theta_i\}$. There are two advantages—it can be generated with a simple quantum circuit and it is convenient to figure out its entropy.

B. Unitary Quantum Neural Network

After preparing the initial state, we demonstrate the unitary quantum neural network applied in our quantum algorithm in detail. As shown in fig(1), the unitary quantum neural network consist of p layers and each layer of the quantum neural network is the combination of a series of one-qubit gates and a series of two-qubit gates. In the l -th layer, the series of one-qubit gates can be described as

$$H_s(\lambda_l, \zeta_l) = H_z(\lambda_l) + H_x(\zeta_l), \quad (13)$$

where

$$H_z(\lambda_l) = \sum_i^N \lambda_{l,i} Z_i, \quad (14)$$

which is parameterized by a variable parameter set $\{\lambda_{l,i}\}$, and

$$H_x(\zeta_l) = \sum_i^N \zeta_{l,i} X_i, \quad (15)$$

which is parameterized by a variable parameter set $\{\zeta_{l,i}\}$. In the same way, The series of two-qubit gates can be described as

$$H_{zz}(\alpha_l) = \sum_i^{N-1} \alpha_{l,i} Z_i Z_{i+1}, \quad (16)$$

which is parameterized by a variable parameter set $\{\alpha_{l,i}\}$. Thus, the unitary quantum neural network with p layers can be given by

$$U(\lambda, \zeta, \alpha) = \prod_{l=1}^p \exp[-i(\lambda_l H_x + \zeta_l H_z + \alpha_l H_{zz})], \quad (17)$$

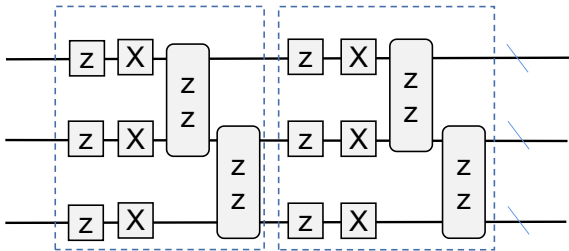


FIG. 1. A depiction of the unitary quantum neural network with 2 layers on a system of three qubits

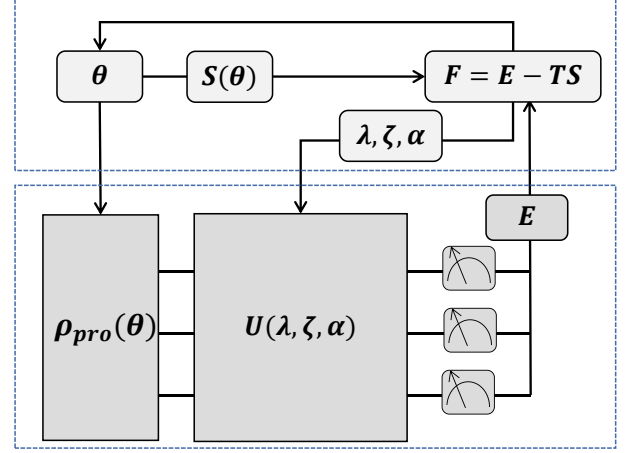


FIG. 2. A pictorial representation of the variational quantum algorithm, which can prepare thermal states and compute the corresponding free energy. In quantum device, we design an initial product state $\rho_{pro}(\theta)$ and the unitary quantum neural network $U(\lambda, \zeta, \alpha)$ parameterized by a series of variable parameters. Using classical computers, the variable parameters $(\theta, \lambda, \zeta, \alpha)$ are updated and optimized in order to minimize the free energy.

In general, the larger number of layer p , the better the quantum neural network can approximate the target state.

C. The flow of the algorithm

As shown in fig(2), our algorithm is a hybrid quantum-classical algorithm which can generate a target quantum mixed state in quantum device with the help of the classical device. In quantum device, we design an initial product state and the unitary quantum neural network parameterized by a series of variable parameters. Then the classical device help to optimize the variable parameters until the target state is achieved. Now, we elaborate our algorithm in detail.

First of all, an initial parameter set θ is got from the classical device and an initial product state $\rho_{pro}(\theta)$ is prepared in quantum device. Then the parameterized unitary quantum neural network is applied. After unitary evolution, we get

$$\rho(\theta, \lambda, \zeta, \alpha) = U(\lambda, \zeta, \alpha) \rho_{pro}(\theta) U^\dagger(\lambda, \zeta, \alpha). \quad (18)$$

Under the unitary operator, the entropy of the quantum mixed state keep invariant

$$\begin{aligned} S(\rho(\theta, \lambda, \zeta, \alpha)) &= S(U(\lambda, \zeta, \alpha) \rho_{pro}(\theta) U^\dagger(\lambda, \zeta, \alpha)) \\ &= S(\rho_{pro}(\theta)). \end{aligned} \quad (19)$$

It is extremely difficult to computing the entropy of $\rho(\theta, \lambda, \zeta, \alpha)$ using the classical device because the computational complexity will increase exponentially with the system size. Fortunately, the Eq.(19) implies that if we want to know the entropy of the quantum mixed state at any moment, we just need to know the entropy of the initial mixed state $\rho_{pro}(\theta)$. With Eq(10) and Eq(12), it is a feasible task for the classical

device to calculate the entropy of $\rho_{pro}(\theta)$, of which the computational complexity just increases linearly with the system size. Notice that our goal is to generate a thermal mixed state according to the hamiltonian H of the quantum system studied. At finite specific temperature, the thermal mixed state is an equilibrium state with the form

$$\rho_{goal} = \frac{1}{Z} e^{-\beta H}, \quad (20)$$

in which Z is the partition function and $\beta = \frac{1}{T}$ is the inverse temperature. At constant temperature T , only when the free energy is minimal, the system is in equilibrium state. So free energy can be used as a criterion to judge whether the system is equilibrium or not. By the moment, our goal becomes to generate a mixed state $\rho(\theta, \lambda, \zeta, \alpha)$ with the minimal free energy. Hence we define the free energy as the cost function in quantum machine learning

$$\begin{aligned} F(\theta, \lambda, \zeta, \alpha) &= E - TS \\ &= \text{tr}[\rho(\theta, \lambda, \zeta, \alpha)H] \\ &\quad - TS(\rho(\theta, \lambda, \zeta, \alpha)). \end{aligned} \quad (21)$$

The first term is the energy of the system, which can get from measurement of the quantum system, as shown in fig(2). From Eq.(19), Eq.(10) and Eq.(12), we can see that the entropy of $\rho(\theta, \lambda, \zeta, \alpha)$ is determined by variable parameter set θ and it is practicable to compute in the classical device. Therefore, the free energy of the quantum mixed state $F(\theta, \lambda, \zeta, \alpha)$ is feasible to figure out in our algorithm even if facing with a large system. Subsequently, variable parameter sets $(\theta, \lambda, \zeta, \alpha)$ is optimized by the gradient descent method in the classical device in order to get the smaller free energy. After many times iterations, the appropriate parameter sets will be obtained which can generate a mixed state with the minimal free energy in quantum device.

IV. RESULT

V. CONCLUSION

VI. CONCLUSION

VII. CONCLUSION

ACKNOWLEDGMENTS

Appendix A: The circuit of subsystem

In this appendix, we detail the circuit of subsystem. As shown in fig(6), prepare the initial state $|00\rangle$ first. Then apply a one-qubit gate $Rx(\theta_i)$ to the first qubit

$$Rx(\theta_i) = \cos(\theta_i)I + \sin(\theta_i)\sigma^x, \quad (A1)$$

We get

$$\begin{aligned} Rx_1(\theta_i) |00\rangle &= \cos(\theta_i)I_1 |00\rangle + \sin(\theta_i)\sigma_1^x |00\rangle \\ &= \cos(\theta_i) |00\rangle + \sin(\theta_i) |10\rangle. \end{aligned} \quad (A2)$$

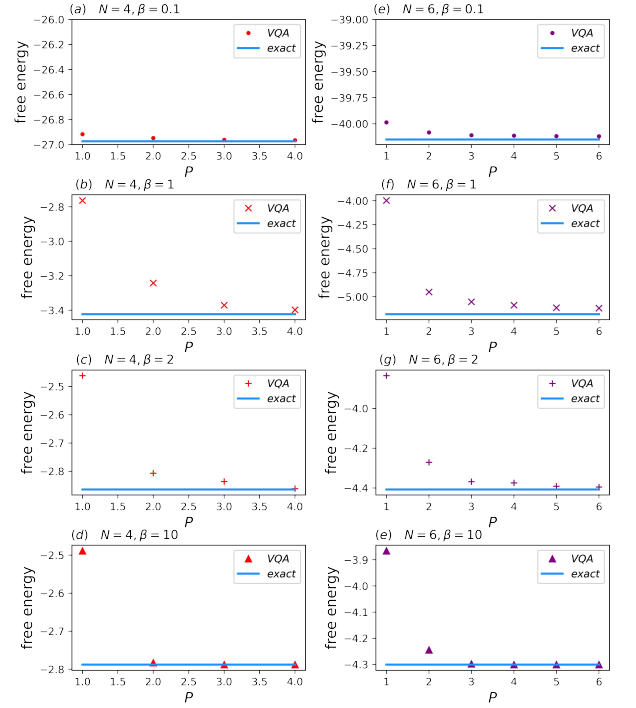


FIG. 3. Comparison of the results of the quantum variational algorithm and exact values at different temperatures. As the layer of quantum circuit P increases, the free energy calculated by the quantum variational algorithm will converge to the exact value.

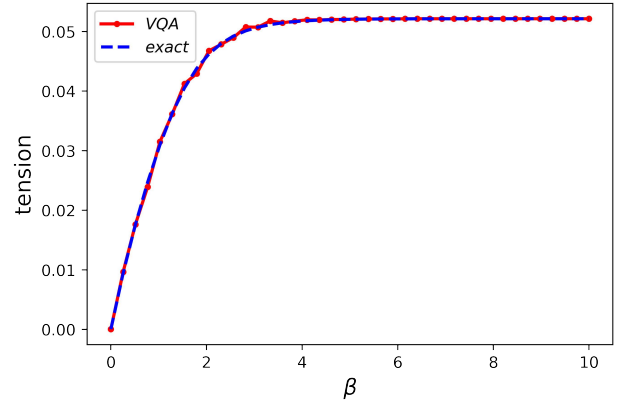


FIG. 4. Unitary Quantum Neural Network

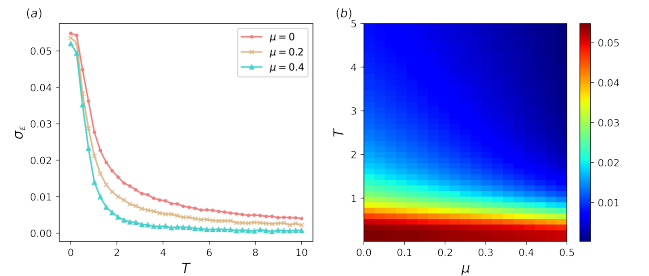


FIG. 5. Unitary Quantum Neural Network

Next, apply a two-qubit gate C-not, we get a entangle state

$$\cos(\theta_i) |00\rangle + \sin(\theta_i) |11\rangle. \quad (\text{A3})$$

Finally, trace out the first qubit, we get a mixed state

$$\rho_{sub} = \sin^2(\theta_i) |0\rangle\langle 0| + \cos^2(\theta_i) |1\rangle\langle 1| \quad (\text{A4})$$

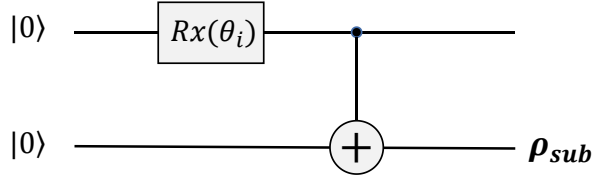


FIG. 6. The circuit of subsystem